Performance of Cumulant Based Inverse Filters for Blind Deconvolution

Chih-Chun Feng, *Student Member, IEEE,* and Chong-Yung Chi, *Senior Member, IEEE*

***Abstract*—Chi and Wu proposed a class of inverse filter criteria $J_{r,m}$ using rth-order and mth-order cumulants (where r is even and $m > r \geq 2$) for blind deconvolution (equalization) of a (nonminimum phase) linear time-invariant (LTI) system with only non-Gaussian measurements. The inverse filter criteria $J_{r,m}$ for $r = 2$ are frequently used such as Wiggins' criterion, Donoho's criteria, and Tugnait's inverse filter criteria for which the identifiability of the LTI system is based on infinite signal-to-noise ratio (SNR). In this paper, we analyze the performance of the inverse filter criteria $J_{2,m}$ $(r = 2)$ when the SNR is finite. The analysis shows that the inverse filter associated with $J_{2,m}$ is related to the minimum mean square error (MMSE) equalizer in a nonlinear manner, with some common properties such as perfect phase (but not perfect amplitude) equalization. Furthermore, the former approaches the latter either for higher SNR, cumulant-order m, or for wider system bandwidth. Moreover, as the MMSE equalizer does, the inverse filter associated with $J_{2,m}$ also performs noise reduction besides equalization. Some simulation results, as well as some calculation results, are provided to support the proposed analytic results.**

***Index Terms*—Blind deconvolution, equalization, higher order statistics, inverse filter criteria.**

I. Introduction

BLIND deconvolution (or blind equalization) is a signal processing procedure that recovers a desired signal $u(n)$ from a given set of measurements

$$x(n) = x_{\mathrm{S}}(n) + w(n) \tag{1}$$

where

$$x_{\mathrm{S}}(n) = u(n) * h(n) = \sum_{k=-\infty}^{\infty} h(k)u(n-k) \tag{2}$$

is the noise-free signal distorted by an unknown linear time-invariant (LTI) system (channel) $h(n)$, and $w(n)$ is the measurement noise accounting for sensor noise as well as physical effects not explained by $x_{\mathrm{S}}(n)$. The problem of blind deconvolution arises comprehensively in various applications such as digital communications, seismic signal processing, speech modeling and synthesis, ultrasonic nondestructive evaluation (NDE), and image restoration.

Manuscript received March 19, 1998; revised January 10, 1999. This work was supported by the National Science Council under Grants NSC-85-2213-E-007-012 and NSC-86-2213-E-007-037. Part of the work in this paper was presented at First IEEE Signal Processing Workshop on Signal Processing Advances in Wireless Communications, Paris, France, April 16–18, 1997. The associate editor coordinating the review of this paper and approving it for publication was Dr. Akram Aldroubi.

The authors are with the Department of Electrical Engineering, National Tsing Hua University, Hsinchu, Taiwan, R.O.C.

Publisher Item Identifier S 1053-587X(99)04684-X.

The conventional linear prediction error (LPE) filter [1]–[4] using second-order statistics (correlations or power spectra) has been widely used in blind deconvolution in the past three decades. The LPE filter, however, is minimum phase with magnitude response proportional to that of the inverse system of $h(n)$. Therefore, when the unknown system $h(n)$ is not minimum phase, phase distortion will remain in the predictive deconvolved signal, and meanwhile, the performance of the LPE filter is sensitive to additive noise simply because correlations of the measurements $x(n)$ are the sum of correlations of the noise-free signal $x_{\mathrm{S}}(n)$ and those of the additive noise $w(n)$. On the other hand, inverse filter criteria [5]–[19] using higher order statistics (cumulants or polyspectra [20]–[25]) have been reported in the past decade for blind deconvolution of nonminimum-phase LTI systems when $x_{\mathrm{S}}(n)$ is non-Gaussian, and $w(n)$ is Gaussian for the following reasons. Higher order (≥ 3) cumulants of the non-Gaussian measurements $x(n)$ contain not only the amplitude but also phase information of the unknown system $h(n)$; furthermore, they are insensitive to Gaussian noise since all higher order (≥ 3) cumulants of Gaussian random processes are equal to zero.

In practical applications, the signal-to-noise ratio (SNR) defined as

$$\mathrm{SNR} = \frac{E\{x_{\mathrm{S}}^2(n)\}}{E\{w^2(n)\}} \quad [\text{see (1)}] \tag{3}$$

may not be very high, and thus, the presence of the measurement noise $w(n)$ may lead to serious effects on the deconvolved (equalized) signal as well as on the behavior of the deconvolution filter (equalizer) for finite SNR. For example, in digital communications, it is well known that the infinite-length zero-forcing (ZF) equalizer [26] can ideally eliminate the intersymbol interference (ISI) induced by the channel distortion, namely, it is a perfect (amplitude and phase) equalizer. However, the ZF equalizer may also significantly amplify the noise power in the equalized signal, thereby leading to high error rate in the following decision procedure for reconstruction of the desired information sequence. On the other hand, the minimum mean square error (MMSE) equalizer [26] is known to perform the ISI and noise reduction simultaneously when SNR is finite.

Let $v(n)$ be an estimate for the inverse system of $h(n)$ and $e(n)$ be the output of the inverse filter $v(n)$ in response to the measurements $x(n)$, i.e.,

$$e(n) = x(n) * v(n). \tag{4}$$

Moreover, let cum$\{x_1, x_2, \ldots, x_m\}$ denote the joint cumulant of random variables $x_1, x_2, \cdots, x_m$. Chi and Wu [5], [6] find the optimum inverse filter $v(n)$ by maximizing

$$J_{r,m}(v(n)) = \frac{|C_m\{e(n)\}|^r}{|C_r\{e(n)\}|^m} \tag{5}$$

where r is even, $m > r \geq 2$, and $C_m\{e(n)\}$ $(C_r\{e(n)\})$ denotes the mth-order (rth-order) cumulant of $e(n)$, i.e.,

$$C_m\{e(n)\} = \text{cum}\{x_1 = e(n), x_2 = e(n), \cdots, x_m = e(n)\}. \tag{6}$$

Similar results about the inverse filter criteria $J_{r,m}$ were also reported in [7]. This class of inverse filter criteria $J_{r,m}$ includes, for example, Wiggins' criterion [8] (associated with $J_{2,4}$), Donoho's criteria [9] (associated with $J_{2,m}$), and Tugnait's criteria $J_{2,3}, J_{2,4}$, and $J_{4,6}$ [10] as special cases. The versions of $J_{2,m}$ for complex signals have been proposed by Shalvi and Weinstein [11], [12] for communication applications.

Chi and Wu [5], [6] proved that under some general assumptions (to be presented in Section II), the inverse filter criteria $J_{r,m}$ given by (5) lead to perfect equalization either when $r = 2$ and SNR $= \infty$ or when $r \geq 4$. In other words, when SNR is finite, the inverse filter $v(n)$ associated with $J_{r,m}$ for $r \geq 4$ is exactly the same as the ZF equalizer, while that associated with $J_{2,m}$, such as Wiggins, Donoho, and Tugnait's inverse filter criteria mentioned above, is not clear for finite SNR. This, therefore, motivated the studies about the behavior of the resultant inverse filter $v(n)$ for $J_{2,m}$ and the studies about the noise reduction performed by the inverse filter $v(n)$ when SNR is finite.

The rest of the paper is organized as follows. Section II presents the model assumptions and briefly reviews the MMSE equalizer for ease of later use. Section III analyzes the behavior of the inverse filter $v(n)$ associated with $J_{2,m}$ for finite SNR. Section IV presents some analytic results about the SNR improvement or degradation after deconvolution. In Section V, some simulation and calculation results are provided to support the proposed analytic results. Finally, some conclusions are drawn in Section VI.

II. Model Assumptions and Review of the MMSE Equalizer

For the non-Gaussian measurements $x(n)$ modeled by (1) and (2), let us make the following assumptions.

- A1) The LTI system $h(n)$, which can be either minimum phase or nonminimum phase, is real stable and its stable inverse system, which is denoted $h_{\rm I}(n)$, exists.
- A2) The desired signal $u(n)$ is a real, zero-mean, independent identically distributed (i.i.d.), non-Gaussian random process with variance σ_u^2 and mth-order cumulant γ_m $(m \geq 3)$.
- A3) The measurement noise $w(n)$ is a real, zero-mean, (white or colored) Gaussian random process that can be modeled as

$$w(n) = \eta(n) * b(n) \tag{7}$$

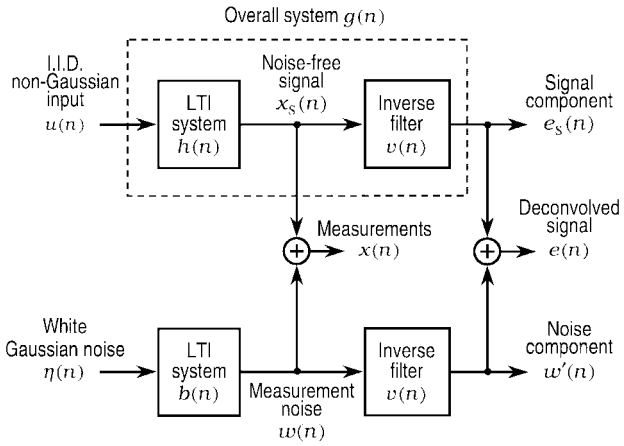

Fig. 1. Block diagram for the interpretation of blind deconvolution using inverse filters.

where $\eta(n)$ is a real white Gaussian noise with variance σ_η^2, and $b(n)$ is a real stable LTI system with its stable inverse system, which is denoted $b_{\rm I}(n)$, being existent.

- A4) The signal $u(n)$ is statistically independent of the noise $\eta(n)$.

For ease of later use, let us further express the deconvolved signal $e(n)$ given by (4) as (see the block diagram in Fig. 1)

$$e(n) = [x_{\rm S}(n) + w(n)] * v(n) = e_{\rm S}(n) + w'(n) \quad \text{[by (1)]} \tag{8}$$

where

$$w'(n) = w(n) * v(n) = \eta(n) * [b(n) * v(n)] \quad \text{[by (7)]} \tag{9}$$

corresponds to the noise component in $e(n)$, and

$$e_{\rm S}(n) = x_{\rm S}(n) * v(n) = u(n) * g(n) \quad \text{[by (2)]} \tag{10}$$

is the corresponding signal component in which

$$g(n) = h(n) * v(n) \tag{11}$$

is the overall system after deconvolution. Next, let us briefly review the MMSE equalizer.

Let $H(\omega), B(\omega), V(\omega)$, and $G(\omega)$ denote the frequency responses of $h(n), b(n), v(n)$, and $g(n)$, respectively. The (infinite-length) MMSE equalizer, which is denoted $v_{\rm MSE}(n)$, which minimizes the mean square error (MSE) $E\{[u(n) - e(n)]^2\}$, is a (noncausal) Wiener deconvolution filter with frequency response given by [4]

$$V_{\rm MSE}(\omega) = \frac{\sigma_u^2 \cdot H^*(\omega)}{\sigma_u^2 \cdot |H(\omega)|^2 + \sigma_\eta^2 \cdot |B(\omega)|^2} \tag{12}$$

where the superscript '*' represents complex conjugation. The corresponding overall system $G(\omega)$ is therefore given by

$$\begin{aligned} G_{\rm MSE}(\omega) &= H(\omega) \cdot V_{\rm MSE}(\omega) \\ &= \frac{\sigma_u^2 \cdot |H(\omega)|^2}{\sigma_u^2 \cdot |H(\omega)|^2 + \sigma_\eta^2 \cdot |B(\omega)|^2}. \end{aligned} \tag{13}$$

Note that when the measurement noise $w(n)$ is white, i.e., $b(n)$ is an allpass system [see (7)], $V_{\rm MSE}(\omega)$, given by (12), is

the same as the frequency response of Mendel's (steady-state) minimum-variance deconvolution (MVD) filter [27]–[29].

By A3), the overall system $G_{\rm MSE}(\omega)$ given by (13) can be further written as

$$G_{\rm MSE}(\omega)=\frac{\sigma_u^2\cdot\left|\dfrac{H(\omega)}{B(\omega)}\right|^2}{\sigma_u^2\cdot\left|\dfrac{H(\omega)}{B(\omega)}\right|^2+\sigma_\eta^2}=\frac{\sigma_u^2\cdot|F(\omega)|^2}{\sigma_u^2\cdot|F(\omega)|^2+\sigma_\eta^2} \tag{14}$$

where $F(\omega)=H(\omega)/B(\omega)$ is the frequency response of the system

$$f(n)=h(n)*b_{\rm I}(n). \tag{15}$$

It can be seen that the overall system $G_{\rm MSE}(\omega)$ given by (13) is equivalent to that of Mendel's MVD filter as given by (14) when the effective system $F(\omega)=H(\omega)$ (i.e., $B(\omega)=1$ and the measurement noise $w(n)=\eta(n)$ is white). Thus, some properties about Mendel's MVD filter reported in [30] and [31] are also shared by the MMSE equalizer $v_{\rm MSE}(n)$ that are summarized as follows.

- R1) The MMSE equalizer $v_{\rm MSE}(n)$ is a perfect phase equalizer since $G_{\rm MSE}(\omega)$ is zero phase [see (13) or (14)].
- R2) When $f(n)$ is an allpass system, the MMSE equalizer $v_{\rm MSE}(n)$ is a perfect (amplitude and phase) equalizer since $G_{\rm MSE}(\omega)$ equals a constant [see (14)].
- R3) The larger SNR is or the wider the bandwidth of $f(n)$ is, the closer $g_{\rm MSE}(n)$ [the inverse Fourier transform of $G_{\rm MSE}(\omega)$] is to $\delta(n)$.
- R4) $g_{\rm MSE}(n)$ is like an autocorrelation function since $g_{\rm MSE}(n)=g_{\rm MSE}(-n)$ and $G_{\rm MSE}(\omega)\geq 0$, and thus, $g_{\rm MSE}(0)\geq|g_{\rm MSE}(n)|$ [3], [4].

Furthermore, it can be shown that

$$g_{\rm MSE}(0)>|g_{\rm MSE}(n)|,\quad \text{for all } n\neq 0. \tag{16}$$

The proof of (16) needs the following theorem.

Theorem 1: Suppose that $r_z(n)$ is the autocorrelation function of a wide-sense stationary random process $z(n)$, i.e., $r_z(n)=E\{z(k)z(k+n)\}$. If $r_z(0)=|r_z(n_0)|$ for some n_0, then $r_z(n)$ is periodic with period equal to either n_0 when $r_z(n_0)>0$ or $2n_0$ when $r_z(n_0)<0$. □

The proof of Theorem 1 is given in Appendix A. Note that Theorem 1 is an extension of the property of autocorrelation functions in [4, p. 84], where only the case of $r_z(n_0)>0$ was considered. Because both the system $h(n)$ and the MMSE equalizer $v_{\rm MSE}(n)$ are stable, the overall system $g_{\rm MSE}(n)$ $(=h(n)*v_{\rm MSE}(n))$ is also stable (i.e., $\Sigma_n\,|g_{\rm MSE}(n)|<\infty$) and, thus, is never a periodic sequence. This fact, together with R4) and Theorem 1, implies that (16) is true.

III. Analysis of the Behavior of the Inverse Filter Associated with $J_{2,m}$

When SNR is finite, the behavior of the inverse filter $v(n)$ associated with the inverse filter criteria $J_{2,m}$ is analyzed in this section. Because the measurement noise $w(n)$ is Gaussian, the mth-order cumulant $C_m\{e(n)\}$ given by (5) can be shown to be [20]–[25]

$$C_m\{e(n)\}=C_m\{e_{\rm S}(n)\}=\gamma_m\sum_{n=-\infty}^{\infty}g^m(n),\qquad m\geq 3. \tag{17}$$

On the other hand, by (8)–(10), $C_r\{e(n)\}$ given by (5) for $r=2$ is known to be [2]–[4]

$$\begin{aligned}C_2\{e(n)\}&=E\{e_{\rm S}(n)^2\}+E\{w'(n)^2\}\\&=\sigma_u^2\sum_{n=-\infty}^{\infty}g^2(n)+\sigma_\eta^2\sum_{n=-\infty}^{\infty}[b(n)*v(n)]^2\\&=\sigma_u^2\sum_{n=-\infty}^{\infty}g^2(n)+\sigma_\eta^2\sum_{n=-\infty}^{\infty}[f_{\rm I}(n)*g(n)]^2\end{aligned} \tag{18}$$

where in the third line, we have used the fact that $v(n)=h_{\rm I}(n)*g(n)$ [see (11)] and that the inverse system of $f(n)$ is given by

$$f_{\rm I}(n)=b(n)*h_{\rm I}(n)\quad[\text{see (15)}]. \tag{19}$$

By (17) and (18), $J_{2,m}$ given by (5) can be written as a function of $g(n)$ as

$$\begin{aligned}J_{2,m}(g(n))=&\frac{|\gamma_m|^2}{|\sigma_u^2|^m}\cdot R_{2,m}(g(n))\\&\cdot\frac{1}{\left|1+\dfrac{\sigma_\eta^2}{\sigma_u^2}\cdot\dfrac{\sum\limits_n[f_{\rm I}(n)*g(n)]^2}{\sum\limits_n g^2(n)}\right|^m}\end{aligned} \tag{20}$$

where

$$R_{2,m}(g(n))=\frac{\left|\sum\limits_n g^m(n)\right|^2}{\left|\sum\limits_n g^2(n)\right|^m}. \tag{21}$$

A remark regarding $R_{2,m}(g(n))$ follows.

- R5) It was shown in [5] and [6] that $0<R_{2,m}(g(n))=R_{2,m}(\alpha g(n-\tau))\leq 1$ and $R_{2,m}(\alpha\delta(n-\tau))=1$ for all $m>2$, where α is a constant, and τ $(-\infty<\tau<\infty)$ is an integer. This result implies that the closer $g(n)$ is to $\delta(n)$ (except for a scale factor and a time delay), the closer $R_{2,m}(g(n))$ is to unity.

Next, let us present the analytic results about the behavior of the inverse filter $v(n)$ associated with $J_{2,m}$.

A. Properties About the Behavior of the Inverse Filter

Assume that the length of the inverse filter $v(n)$ is doubly infinite; thereby, the analysis of the behavior of $v(n)$ can be performed by investigating the behavior of the overall system $g(n)$ without the influence caused by finite-length truncation of $v(n)$ [12].

Property 1: The overall system $g(n)$ associated with $J_{2,m}$ is a linear-phase system, i.e.,

$$\Phi(\omega) \triangleq \arg[G(\omega)] = -\omega\xi + \pi L, \qquad -\pi \le \omega < \pi \quad (22)$$

where ξ is a constant, and L is an integer. □

See Appendix B for the proof of Property 1. This property implies that the associated inverse filter $v(n)$ completely cancels (equalizes) the system phase response of $h(n)$ (uniquely defined up to a linear phase term) and thus, like the MMSE equalizer [see R1)], it performs as a perfect phase equalizer (except for an unknown time delay).

According to Property 1, let $g_{\mathrm{ZP}}(n)$ be a zero-phase version of $g(n)$ as

$$g_{\mathrm{ZP}}(n) = e^{-j\pi L} \cdot g(n+\xi) \quad (23)$$

(with the sign ambiguity and time delay in $g(n)$ removed), and $G_{\mathrm{ZP}}(\omega)$ denote its Fourier transform. From (22) and (23), we can see that $G_{\mathrm{ZP}}(\omega) = |G(\omega)| \ge 0$. Accordingly, similar to $g_{\mathrm{MSE}}(n)$ [see R4) and (16)], it can be easily shown that $g_{\mathrm{ZP}}(n)$ possesses the following property.

Property 2: The zero-phase system $g_{\mathrm{ZP}}(n)$ given by (23) is like an autocorrelation function with

$$g_{\mathrm{ZP}}(0) > |g_{\mathrm{ZP}}(n)|, \quad \text{for all } n \ne 0. \quad (24)$$

□

This property exhibits the waveshape of $g_{\mathrm{ZP}}(n)$ [or, equivalently, $g(n)$]; specifically, $g_{\mathrm{ZP}}(n)$ has a unique maximum at origin $(n = 0)$ and is symmetric about the origin. These observations thus account for zero-phase patterns in the deconvolved signal $e(n)$ when $u(n)$ is a non-Gaussian sparse spike train as in seismic deconvolution because

$$e_{\mathrm{S}}(n) = e^{j\pi L} \cdot u(n-\xi) * g_{\mathrm{ZP}}(n) \quad [\text{by (10) and (23)}] \quad (25)$$

Meanwhile, the resolution of $e_{\mathrm{S}}(n)$ is determined by the width of the wavelet $g_{\mathrm{ZP}}(n)$.

Next, a connection between the inverse filter and the MMSE equalizer is established as follows.

Property 3: The overall system $g(n)$ associated with $J_{2,m}$ is related to $g_{\mathrm{MSE}}(n)$ via

$$g(n) = \beta \cdot [g(n)]^{m-1} * g_{\mathrm{MSE}}(n) \quad (26)$$

or, in the frequency domain

$$G(\omega) = \beta \cdot G^{(m-1)}(\omega) \cdot G_{\mathrm{MSE}}(\omega) \quad (27)$$

where $\beta \ne 0$ is a constant, and

$$G^{(m-1)}(\omega) \triangleq \underbrace{G(\omega) * G(\omega) * \cdots * G(\omega)}_{(m-1)\text{ terms}}. \quad (28)$$

□

See Appendix C for the proof of this property.

From Property 3, more observations about the relation between the inverse filter and the MMSE equalizer can be discovered as follows.

Property 4: The overall system $g(n)$ associated with $J_{2,m}$ approaches $g_{\mathrm{MSE}}(n)$ (except for a scale factor and a time delay) as either SNR or the cumulant order m increases or as the system $f(n)$ has wider bandwidth. □

Appendix D provides an inference (but not rigorous proof) of this property. The results of Property 4 can be further examined by considering the following three limiting cases:

i) SNR $= \infty$.
ii) $m = \infty$.
iii) $f(n)$ is an allpass system.

When SNR $= \infty$, $J_{2,m} = [|\gamma_m|^2/|\sigma_u^2|^m] \cdot R_{2,m}$ [by (20)] that, together with R5) and (13), leads to the optimum $g(n) = g_{\mathrm{MSE}}(n) = \delta(n)$ (except for a scale factor and a time delay). When $m = \infty$, $[g(n)]^{m-1} = \alpha\delta(n-\xi)$ [due to (23) and (24)], where α is a constant, and thus, $g(n) = \beta\alpha \cdot g_{\mathrm{MSE}}(n-\xi)$ [by (26)]. For the third case, the corresponding results are summarized in the following fact (see Appendix E for the proof).

F1) When $f(n)$ is an allpass system, $g(n) = g_{\mathrm{MSE}}(n) = \delta(n)$ (except for a scale factor and a time delay). In other words, like the MMSE equalizer [see R2)], the associated inverse filter $v(n)$ is also a perfect equalizer, regardless of the values of SNR and m.

B. Algorithm for Computing the Analytic Overall System

To efficiently verify the proposed analytic results, let us present the following FFT-based iterative algorithm for obtaining the overall system $g(n)$ associated with $J_{2,m}$ from $G_{\mathrm{MSE}}(\omega)$ given by (13) according to Property 3.

Algorithm 1:

S1) Set $i = 0$, and choose an initial guess $g_0(n)$ for $g(n)$.
S2) Set $i = i + 1$. Compute the N-point DFT of $[g_{i-1}(n)]^{m-1}$, which is denoted $G_{i-1}^{(m-1)}(\omega_k = 2\pi k/N)$, using FFT.
S3) Compute

$$\tilde{G}_i(\omega_k) = G_{i-1}^{(m-1)}(\omega_k) \cdot G_{\mathrm{MSE}}(\omega_k) \quad [\text{see (27)}] \quad (29)$$

and then compute the N-point inverse DFT of $\tilde{G}_i(\omega_k)$, which is denoted $\tilde{g}_i(n)$, using FFT.
S4) Compute

$$g_i(n) = \frac{\tilde{g}_i(n)}{\sqrt{\sum_n [\tilde{g}_i(n)]^2}}. \quad (30)$$

S5) If $\sum_n [g_i(n) - g_{i-1}(n)]^2 > \epsilon$ (a preassigned tolerance for convergence), then go to S2); otherwise, the analytic overall system $g(n) = g_i(n)$ is obtained.

Some worthy remarks regarding Algorithm 1 are given as follows.

R6) If the initial condition $g_0(n)$ is chosen to be a stable linear phase system, then the analytic overall system $g(n)$ obtained by Algorithm 1 is guaranteed to possess Properties 1 and 2; see Appendix F for the proof.
R7) Gradient-type optimization algorithms [32] can also be used to find a local maximum of $J_{2,m}$ and the

relevant solution for $g(n)$. However, when the length of $g(n)$ is large, these algorithms become impractical because of extraordinary computational load. On the other hand, the FFT length N of Algorithm 1 can be chosen sufficiently large such that aliasing effects on the resultant $g(n)$ are negligible. In other words, Algorithm 1 is never limited by the length of $g(n)$.

IV. Analysis of the SNR Improvement or Degradation After Deconvolution

In this section, let us present the analytic results about the SNR improvement or degradation ratio after deconvolution defined as

$$\rho = \frac{\text{SNR}'}{\text{SNR}} \tag{31}$$

where SNR$'$ denotes the SNR in the deconvolved signal $e(n)$, i.e.,

$$\text{SNR}' = \frac{E\{e_{\text{S}}(n)^2\}}{E\{w'(n)^2\}} \quad \text{[see (8)]}. \tag{32}$$

Note that $\rho > 1$ indicates the SNR improvement after deconvolution, whereas $\rho < 1$ indicates the SNR degradation after deconvolution.

It can be seen, from (18), that SNR$'$ defined by (32) can be further expressed as

$$\text{SNR}' = \frac{\sigma_u^2 \sum_n g^2(n)}{\sigma_\eta^2 \sum_n [f_{\text{I}}(n) * g(n)]^2} \tag{33}$$

which reveals that SNR$'$ depends on $g(n)$ [or, equivalently, $v(n)$], and so does the ratio ρ [since (31)]. Therefore, for clarity, let $\rho_{\text{ZF}}, \rho_{\text{MSE}}$ and $\rho_{2,m}$ denote the values of ρ for the ZF equalizer, the MMSE equalizer, and the inverse filter $v(n)$ associated with $J_{2,m}$, respectively. Two facts regarding ρ_{ZF} and ρ_{MSE} are described as follows: (see Appendix G for the proof)

F2) If the measurement noise $w(n)$ is white, $\rho_{\text{ZF}} \le 1$; otherwise, ρ_{ZF} can be greater than unity. In other words, the ZF equalizer always leads to the SNR degradation after deconvolution when $w(n)$ is white.

F3) The ratio $\rho_{\text{MSE}} \ge \rho_{\text{ZF}}$, implying that the MMSE equalizer performs noise reduction better than the ZF equalizer.

Let us rewrite $J_{2,m}$ given by (20) as a function of $g(n)$ and $\rho_{2,m}$ as

$$J_{2,m}(g(n), \rho_{2,m}) = \frac{|\gamma_m|^2}{|\sigma_u^2|^m} \cdot R_{2,m}(g(n)) \cdot \frac{1}{\left|1 + \dfrac{1}{\rho_{2,m} \cdot \text{SNR}}\right|^m} \quad \text{[by (33) and (31)]}. \tag{34}$$

We can easily observe, from (34), that the optimum $g(n)$ associated with the maximum of $J_{2,m}$ partly maximizes $R_{2,m}(g(n))$ for the ISI reduction [see R5)] and partly maximizes $\rho_{2,m}$ for noise reduction in the meantime. In other words, as the MMSE equalizer does, the inverse filter $v(n)$ associated with $J_{2,m}$ also performs noise reduction besides the ISI reduction. Furthermore, as the former does [see F3)], the latter also performs noise reduction better than the ZF equalizer, as exhibited by the following property.

Property 5: The ratio $\rho_{2,m} \ge \rho_{\text{ZF}}$. □

See Appendix H for the proof of Property 5.

Moreover, according to Property 4, the following results can be easily inferred:

Property 6: The ratio $\rho_{2,m}$ approaches ρ_{MSE} as either SNR or the cumulant order m increases or as the system $f(n)$ has wider bandwidth. □

This property also supports the above-mentioned facts about the noise reduction performed by the inverse filter. In addition, a further inference about $\rho_{2,m}$ with respect to SNR is as follows:

Property 7: The ratio $\rho_{2,m}$ always increases as SNR decreases. □

See Appendix I for the inference of Property 7. In other words, the lower SNR is, the more the inverse filter $v(n)$ associated with $J_{2,m}$ performs as a noise reduction filter.

V. Simulation and Calculation Results

In this section, let us present three examples to demonstrate the preceding analytic results as well as the proposed FFT-based iterative algorithm (Algorithm 1) for obtaining the analytic overall system $g(n)$ associated with $J_{2,m}$.

Example 1: In this example, the desired signal $u(n)$ was assumed to be a zero-mean, i.i.d., exponential random sequence with variance $\sigma_u^2 = 1$ and skewness $\gamma_3 = 2$. The system $h(n)$ with transfer function

$$H(z) = \frac{1 - 2.7z^{-1} + 0.5z^{-2}}{1 + 0.1z^{-1} - 0.12z^{-2}}$$

(taken from [6, Example 1]) was used. The noisy data $x(n)$ were generated using (1), (2), and (7), where two different systems for $b(n)$ (i.e., $B(z) = 1 + 0.8z^{-1}$ and $B(z) = 1 - 0.8z^{-1}$) were considered. The inverse filter $v(n)$ was approximated by a causal FIR filter $\hat{v}(n)$ of order equal to 16. The criterion $J_{2,3}$ (i.e., $m = 3$) was used with the two cumulants $C_3\{e(n)\}$ and $C_2\{e(n)\}$ [see (5)] replaced by the associated sample cumulants [20]–[25]. The Fletcher–Powell optimization algorithm (an iterative gradient-type optimization algorithm [32]) was used to find the (local) maximum of $J_{2,3}$ and the relevant estimate $\hat{v}(n)$ as well as $\hat{g}(n) = h(n) * \hat{v}(n)$, where $\hat{v}(n) = \delta(n - 8)$ was used to initialize the Fletcher–Powell optimization algorithm. Thirty independent runs were performed with data length equal to 2048 and SNR $= 0$ dB. On the other hand, the analytic overall system $g(n)$ was also calculated using Algorithm 1 with $g_0(n) = g_{\text{MSE}}(n)$ [according to R6) and R1)], the FFT length $N = 1024$, and the convergence tolerance $\epsilon = 10^{-5}$.

Fig. 2(a) shows the average (dashed line) $\pm$ one standard deviation (dotted lines) of the obtained 30 $\hat{g}(n)$'s together with

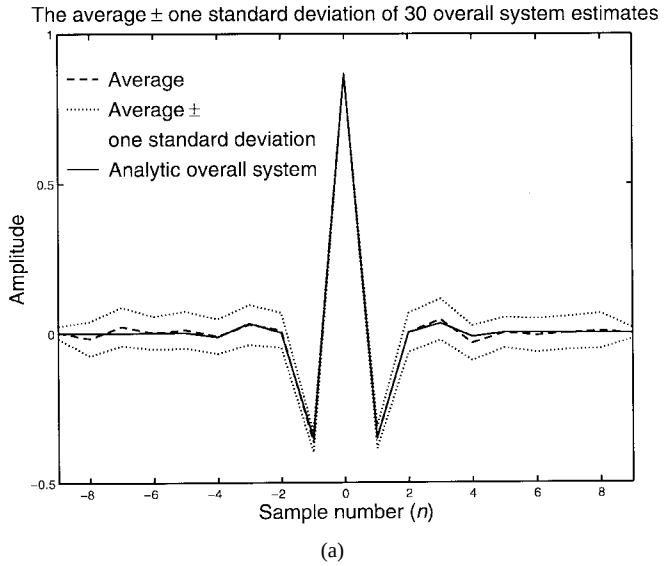

(a)

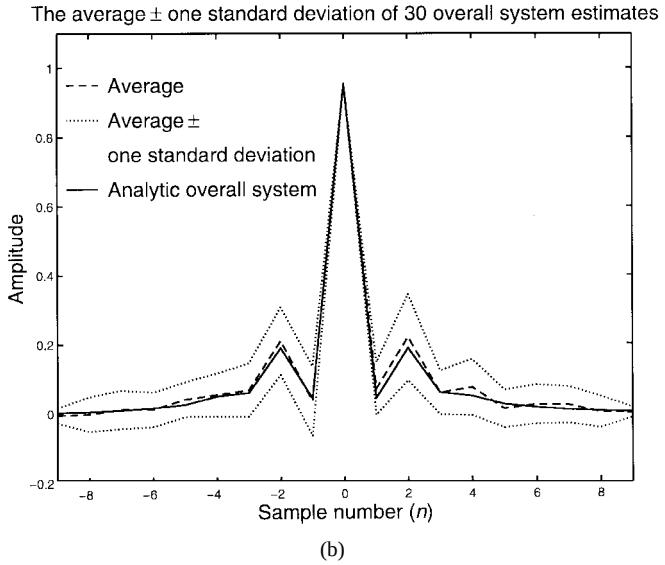

(b)

Fig. 2. Simulation and calculation results of Example 1. (a) Average (dashed line) ± one standard deviation (dotted lines) of the obtained 30 overall system estimates $\hat{g}(n)$'s together with the analytic overall system $g(n)$ (solid line) obtained using Algorithm 1 for $B(z) = 1+0.8z^{-1}$. (b) Results corresponding to part (a) for $B(z) = 1 - 0.8z^{-1}$.

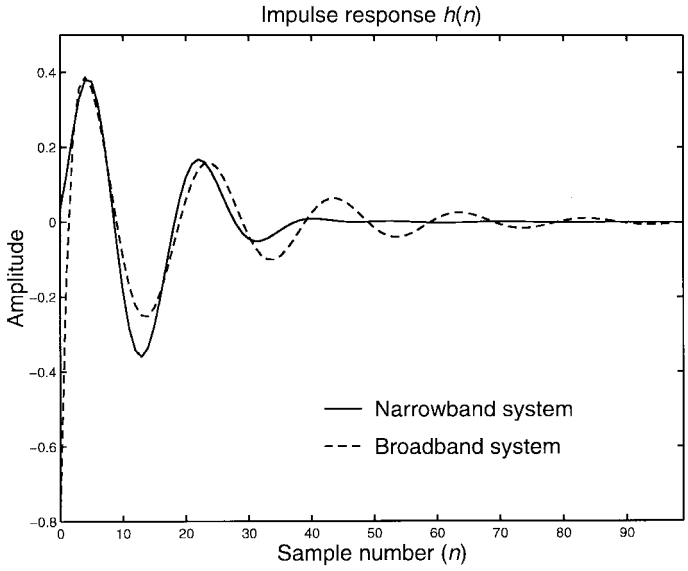

(a)

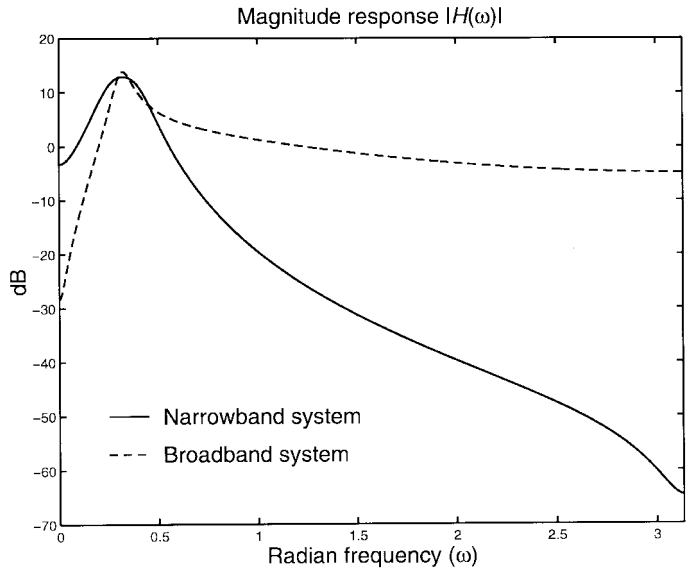

(b)

Fig. 3. Systems used in Example 2. (a) Impulse responses $h(n)$'s. (b) Magnitude responses $|H(\omega)|$'s (in decibels) of the narrowband system (solid lines) and the broadband system (dashed lines), respectively.

the analytic $g(n)$ (solid line) for $B(z) = 1+0.8z^{-1}$ (a lowpass system), where all the scale factors and time delays between $\hat{g}(n)$ and the analytic $g(n)$ have been artificially removed. Fig. 2(b) shows the results corresponding to those shown in Fig. 2(a) for $B(z) = 1 - 0.8z^{-1}$ (a highpass system). We can see, from Fig. 2(a) and (b), that as predicted in Properties 1 and 2, $\hat{g}(n)$ is approximately zero-phase (symmetric) and $\hat{g}(0) > |\hat{g}(n)|, n \neq 0$. Moreover, $\hat{g}(n)$ approximates the analytic $g(n)$ well in spite of the low SNR (0 dB). These results also reveal that the analytic $g(n)$ obtained by Algorithm 1 can serve as a good prediction for $\hat{g}(n)$.

Example 2: In this example, let us only show the calculation results associated with the analytic $g(n)$. A minimum-phase narrowband ARMA(4,2) system taken from [30] and a nonminimum-phase broadband ARMA(4,3) system taken from [33]–[36] for the system $h(n)$ were considered, and the system $b(n) = \delta(n)$ [i.e., $w(n)$ is white] was used. Fig. 3(a) and (b) depict the impulse responses $h(n)$'s and the magnitude responses $|H(\omega)|$'s (in decibels) (i.e., $20\log_{10}|H(\omega)|$) of the narrowband system (solid lines) and the broadband system (dashed lines), respectively. The analytic $g(n)$ was obtained using Algorithm 1 with $g_0(n) = g_{\mathrm{MSE}}(n)$, the FFT length $N = 1024$, and the convergence tolerance $\epsilon = 10^{-5}$.

For the narrowband system, Fig. 4(a) displays the magnitude responses $|G(\omega)|$'s associated with $J_{2,3}, J_{2,4}, J_{2,5}$, and $J_{2,6}$ (short-dash dot, long-dash dot, short-dash and long-dash lines, respectively) together with the associated $G_{\mathrm{MSE}}(\omega)$ (solid line) for SNR $= 30$ dB, where scale factors were artificially removed. The corresponding results for SNR $= 40$ dB are displayed in Fig. 4(b). Note that in Fig. 4(b), the long-dash line and the solid line almost overlap each other. From

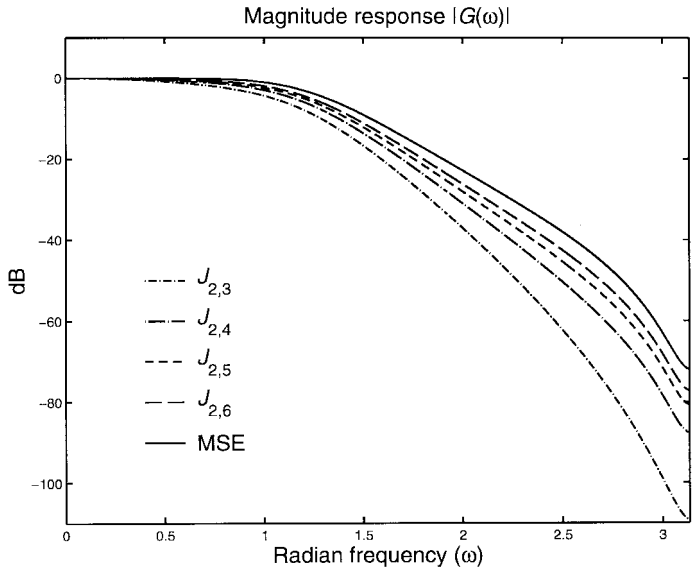

(a)

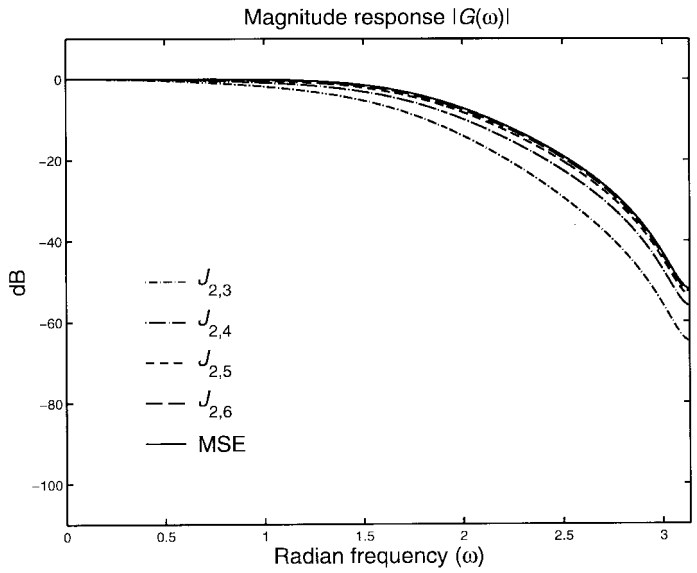

(b)

Fig. 4. Calculation results of Example 2 for the narrowband system. (a) Magnitude responses $|G(\omega)|$'s associated with $J_{2,3}, J_{2,4}, J_{2,5}$, and $J_{2,6}$ (short-dash dot, long-dash dot, short-dash and long-dash lines, respectively) together with the associated $G_{\mathrm{MSE}}(\omega)$ (solid line) for SNR = 30 dB. (b) Results corresponding to part (a) for SNR = 40 dB.

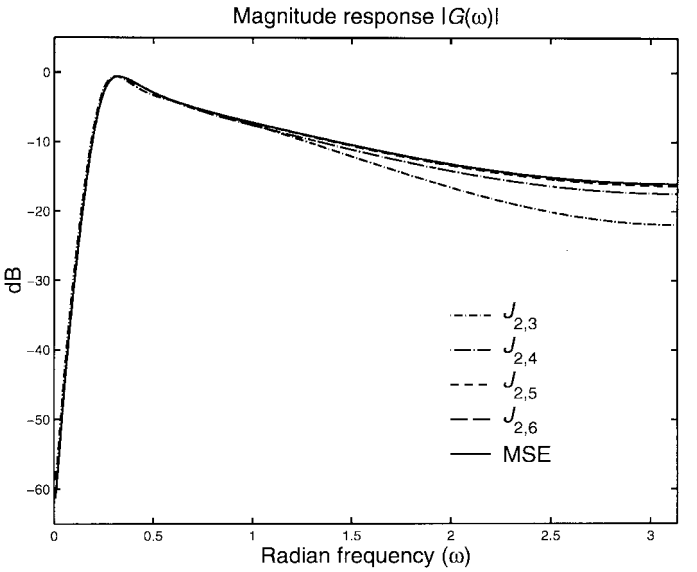

(a)

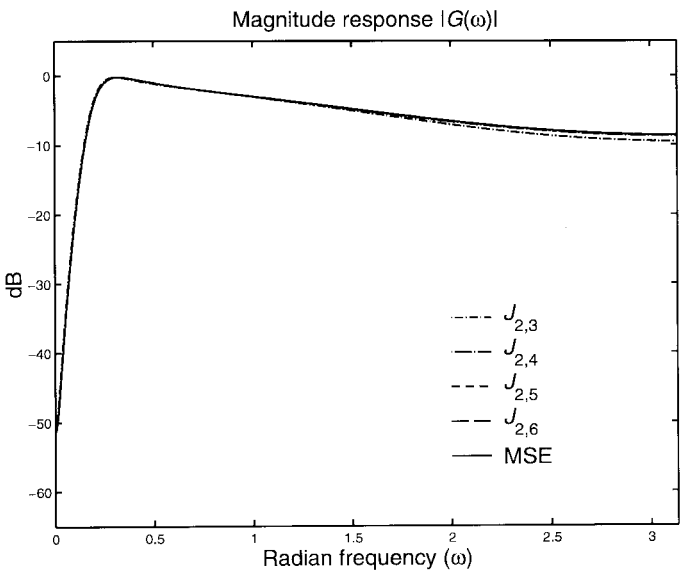

(b)

Fig. 5. Calculation results of Example 2 for the broadband system. (a) Magnitude responses $|G(\omega)|$'s associated with $J_{2,3}, J_{2,4}, J_{2,5}$, and $J_{2,6}$ (short-dash dot, long-dash dot, short-dash and long-dash lines, respectively) together with the associated $G_{\mathrm{MSE}}(\omega)$ (solid line) for SNR = 0 dB. (b) Results corresponding to part (a) for SNR = 5 dB.

Fig. 4(a) and (b), we can see that as predicted in Property 4, $|G(\omega)|$ can be viewed as a better approximation to $G_{\mathrm{MSE}}(\omega)$ for either larger m or higher SNR.

For the broadband system, the results corresponding to those in Fig. 4(a) and (b) are depicted in Fig. 5(a) and (b), respectively, for SNR = 0 dB and 5 dB instead. Again, these results are consistent with Property 4. Moreover, from Figs. 4(a) and 5(a), 4(b), and 5(b), we can see that $|G(\omega)|$ can also be viewed as a better approximation to $G_{\mathrm{MSE}}(\omega)$ for the broadband system than for the narrowband system, in spite of much lower SNR (0 and 5 dB) for the broadband system. These results exhibit that the closeness of the inverse filter associated with $J_{2,m}$ to the MMSE equalizer depends heavily on the bandwidth of the system $h(n)$ and slightly on the value of SNR for this case.

Table I lists the ratios $\rho_{2,3}, \rho_{2,4}, \rho_{2,5}, \rho_{2,6}, \rho_{\mathrm{MSE}}$, and ρ_{ZF} and the corresponding SNR$'$s (in decibels) for the narrowband system. The corresponding results for the broadband system are listed in Table II. We can see, from Tables I and II, that the values of $\rho_{2,m}, m = 3, 4, 5$, and 6 are close to those of ρ_{MSE} and better for higher SNR. Furthermore, the former are closer to the latter for the broadband system than for the narrowband system. These observations support Property 6 since $f(n) = h(n)$ [see (15)] for the white noise case in this example. Moreover, as predicted by Property 7, the values of $\rho_{2,m}, m = 3, 4, 5$, and 6 increase as SNR decreases.

TABLE I
CALCULATION RESULTS OF EXAMPLE 2 FOR THE NARROWBAND SYSTEM. THE RATIOS $\rho_{2,3}, \rho_{2,4}, \rho_{2,5}, \rho_{2,6}, \rho_{\mathrm{MSE}}$, AND ρ_{ZF} AND THE CORRESPONDING SNR'S (IN DECIBELS)

		SNR				
Criterion		40 dB	30 dB	20 dB	10 dB	0 dB
$J_{2,3}$	SNR′ (dB)	12.8534	12.8054	12.6803	9.8840	3.9761
	$\rho_{2,3}$	0.0019	0.0191	0.1854	0.9736	2.4981
$J_{2,4}$	SNR′ (dB)	10.1072	10.9232	10.9453	9.1882	5.0111
	$\rho_{2,4}$	0.0010	0.0124	0.1243	0.8295	3.1704
$J_{2,5}$	SNR′ (dB)	9.0116	9.9040	10.1114	8.7127	4.4307
	$\rho_{2,5}$	7.7965×10^{-4}	0.0098	0.1026	0.7435	2.7737
$J_{2,6}$	SNR′ (dB)	8.6084	9.1813	9.6217	8.4203	4.5005
	$\rho_{2,6}$	7.2583×10^{-4}	0.0083	0.0917	0.6951	2.8187
MSE	SNR′ (dB)	8.3439	7.6930	7.6688	7.0468	4.0761
	ρ_{MSE}	6.8295×10^{-4}	0.0059	0.0585	0.5066	2.5563
ZF	SNR′ (dB)	−12.8243	−22.8243	−32.8243	−42.8243	−52.8243
	ρ_{ZF}			5.2188×10^{-6}		

TABLE II
CALCULATION RESULTS OF EXAMPLE 2 FOR THE BROADBAND SYSTEM. THE RATIOS $\rho_{2,3}, \rho_{2,4}, \rho_{2,5}, \rho_{2,6}, \rho_{\mathrm{MSE}}$, AND ρ_{ZF} AND THE CORRESPONDING SNR'S (IN DECIBELS)

		SNR				
Criterion		40 dB	30 dB	20 dB	10 dB	0 dB
$J_{2,3}$	SNR′ (dB)	28.7695	21.1127	14.4796	6.1343	0.4967
	$\rho_{2,3}$	0.0753	0.1292	0.2805	0.4106	1.1212
$J_{2,4}$	SNR′ (dB)	28.7699	21.1229	14.5028	6.1498	−0.1751
	$\rho_{2,4}$	0.0753	0.1295	0.2820	0.4121	0.9605
$J_{2,5}$	SNR′ (dB)	28.7699	21.1228	14.5022	6.1472	−0.4894
	$\rho_{2,5}$	0.0753	0.1295	0.2820	0.4118	0.8934
$J_{2,6}$	SNR′ (dB)	28.7699	21.1228	14.5023	6.1473	−0.5471
	$\rho_{2,6}$	0.0753	0.1295	0.2820	0.4118	0.8816
MSE	SNR′ (dB)	28.7699	21.1228	14.5023	6.1473	−0.5741
	ρ_{MSE}	0.0753	0.1295	0.2820	0.4118	0.8762
ZF	SNR′ (dB)	28.3147	18.3147	8.3147	−1.6853	−11.6853
	ρ_{ZF}			0.0678		

On the other hand, the values of ρ_{ZF} in Tables I and II are not only much smaller than unity [as mentioned in F2)] but also smaller than those of ρ_{MSE} [as mentioned in F3)] and $\rho_{2,m}, m = 3, 4, 5$, and 6 (as predicted by Property 5). In addition, some values of ρ_{MSE} and $\rho_{2,m}, m = 3, 4, 5$, and 6 are larger than unity (see the last column of Table I and the last column of Table II for $\rho_{2,3}$). These observations indicate that the inverse filter associated with $J_{2,m}$ as well as the MMSE equalizer performs not only as an ISI reduction filter but also as a noise reduction filter, particularly when SNR is low, whereas the ZF equalizer performs as a perfect ISI removal filter despite the tremendous SNR degradation in the deconvolved signal for this case.

Example 3—Seismic Deconvolution: As mentioned in Section III, $u(n)$ is a non-Gaussian sparse reflectivity sequence in seismic deconvolution that can be modeled as a Bernoulli–Gaussian (B-G) sequence [33]–[36], as

$$u(n) = q(n) \cdot r(n)$$

where $q(n)$ is a Bernoulli sequence with parameter λ, i.e.,

$$\Pr[q(n)] = \begin{cases} \lambda, & q(n) = 1 \\ 1 - \lambda, & q(n) = 0 \end{cases}$$

and $r(n)$ is a zero-mean white Gaussian random process with variance σ_r^2. Note that $\sigma_u^2 = \sigma_r^2 \lambda, \gamma_3 = 0$, and $\gamma_4 = 3\sigma_r^2 \lambda(1 - \lambda)$ for the B-G sequence.

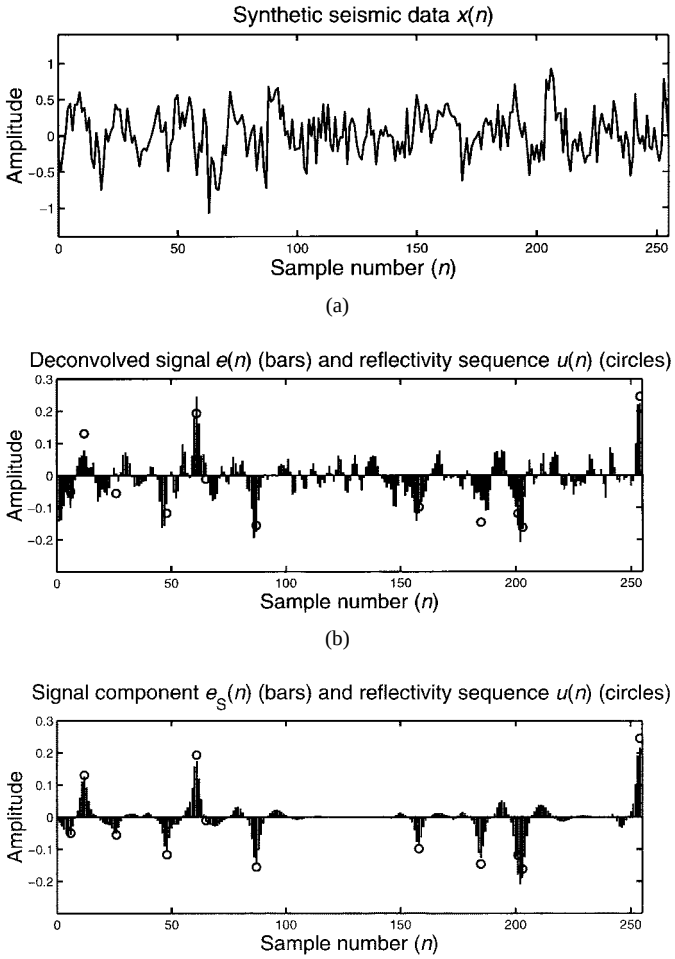

Fig. 6. Simulation results of Example 3 for SNR = 0 dB. (a) Segment $(n = 0 \sim 255)$ of the synthetic seismic data $x(n)$. (b) Deconvolved signal $e(n)$ (bars). (c) Corresponding signal component $e_{\rm S}(n)$ (bars) together with the true reflectivity sequence $u(n)$ (circles).

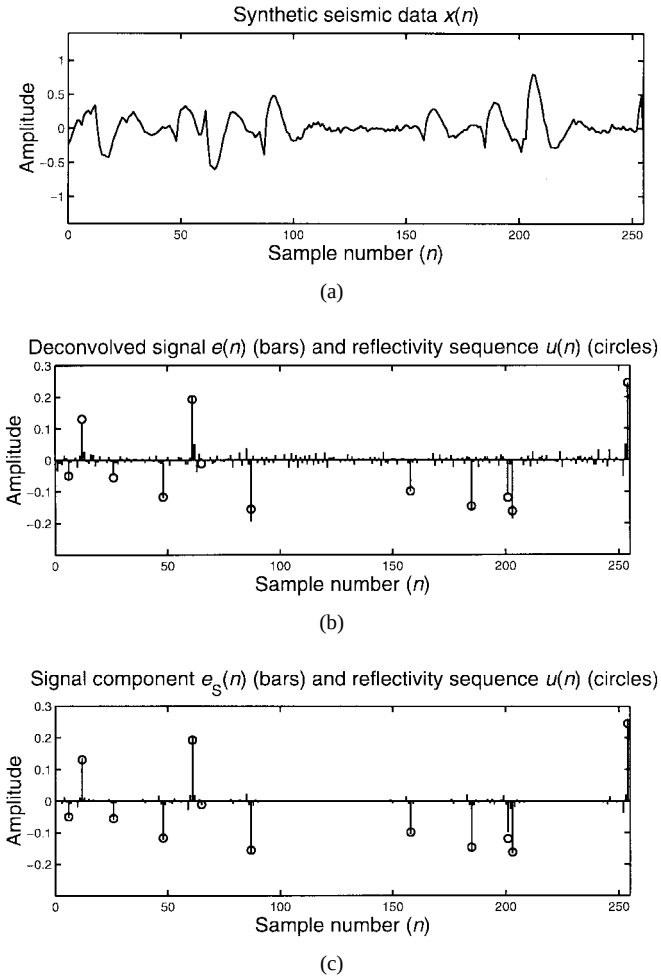

Fig. 7. Simulation results of Example 3 for SNR = 20 dB. (a) Segment $(n = 0 \sim 255)$ of the synthetic seismic data $x(n)$. (b) Deconvolved signal $e(n)$ (bars). (c) Corresponding signal component $e_{\rm S}(n)$ (bars) together with the true reflectivity sequence $u(n)$ (circles).

The noise-free synthetic data $x_{\rm S}(n)$ were generated by convolving a B-G sequence (with $\lambda = 0.05$ and $\sigma_r^2 = 0.0225$) with a third-order nonminimum-phase wavelet $h(n)$ (taken from [6, Example 2]) whose transfer function is given by

$$H(z) = \frac{1 + 0.1z^{-1} - 3.2725z^{-2} + 1.41125z^{-3}}{1 - 1.9z^{-1} + 1.1525z^{-2} - 0.1625z^{-3}.}$$

Then. the synthetic seismic data $x(n)$ were obtained by adding a white Gaussian noise $w(n)$ to the synthetic $x_{\rm S}(n)$. The Fletcher–Powell optimization algorithm was used to find the (local) maximum of $J_{2,4}$ (i.e., $m = 4$) and the relevant inverse filter estimate $\hat{v}(n)$, where $\hat{v}(n)$ was assumed to be a 16th-order causal FIR filter, and the initial condition $\hat{v}(n) = \delta(n - 8)$ was used. A single run was performed for data length equal to 4096 and SNR = 0 and 20 dB.

Fig. 6(a) displays a segment $(n = 0 \sim 255)$ of the synthetic seismic data $x(n)$ for SNR = 0 dB. Fig. 6(b) and (c) display the deconvolved signal $e(n)$ (bars) and the corresponding signal component $e_{\rm S}(n)$ (bars), respectively, together with the true sparse reflectivity sequence $u(n)$ (circles). We can see, from Fig. 6(c), that as the discussion about Property 2 and $e_{\rm S}(n)$ given by (25) in Section III, $e_{\rm S}(n)$ consists of approximate zero-phase wavelets $\hat{g}(n)$'s with amplitudes proportional to $u(n)$, where $\hat{g}(n) = h(n) * \hat{v}(n)$. Note, from Fig. 6(b) and (c), that the two close spikes at $n = 200$ and $n = 202$ are not discernible because the spacing between the two spikes is much narrower than the width of $\hat{g}(n)$ for this case (SNR = 0 dB). Fig. 7(a)–(c) shows the results corresponding to that in Fig. 6(a)–(c), respectively, for SNR = 20 dB. We can see that the deconvolved signal $e(n)$ in Fig. 7(b) is a much better approximation to $u(n)$ than that in Fig. 6(b) due to higher SNR. Moreover, from Fig. 7(b) and (c), we can observe that the two close spikes at $n = 200$ and $n = 202$ are now resolvable simply because the width of $\hat{g}(n)$ is narrower than their spacing for this case (SNR = 20 dB).

VI. Conclusions

We have presented a performance analysis for the inverse filter criteria $J_{2,m}$ given by (5), where $m > 2$ when SNR is finite. The performance analysis was conducted by investigating the behavior of the relevant overall system $g(n)$ and the SNR improvement or degradation ratio $\rho_{2,m}$ after deconvolution [see

(31)]. Seven properties for $J_{2,m}$ were presented in terms of SNR, the cumulant order m, the bandwidth of the system $f(n)$, and the ratio $\rho_{2,m}$. It is almost formidable to find a closed-form solution for the overall system $g(n)$ from the highly nonlinear function $J_{2,m}$ given by (20). The proposed FFT-based iterative algorithm (Algorithm 1) is a computationally efficient method for obtaining the analytic overall system $g(n)$ from $G_{\rm MSE}(\omega)$ given by (13), and the obtained $g(n)$ can then be used to verify the proposed analytic results.

We would like to emphasize that not only the ISI but also the SNR improvement or degradation ratio ρ should be considered as performance measures for deconvolution algorithms. Although the inverse filter associated with $J_{r,m}$ $(r \geq 4)$ is a perfect equalizer for finite SNR, the signal component $e_{\rm S}(n)$ in the deconvolved signal may be invisible due to low SNR$'$ [see (32)]. Properties 5 through 7 suggest that $J_{2,m}$ is preferable to $J_{r,m}$ $(r \geq 4)$ for deconvolution. As a final remark, the presented analytic results are also helpful in the interpretation of the deconvolved signals using $J_{2,m}$.

Appendix A
Proof of Theorem 1

Let us use the cosine inequality [4, p. 67] as

$$\begin{aligned}[E\{z(k)[z(k+n)-\text{sign}(r_z(n_0))\cdot z(k+n+n_0)]\}]^2 \\ \leq E\{z^2(k)\}\cdot E\{[z(k+n)-\text{sign}(r_z(n_0)) \\ \cdot z(k+n+n_0)]^2\}\end{aligned} \tag{A.1}$$

where $\text{sign}(a)=1$ if $a>0$ and -1 if $a<0$. The inequality (A.1) can be further shown to be

$$\begin{aligned}[r_z(n)-\text{sign}(r_z(n_0))\cdot r_z(n+n_0)]^2 \\ \leq 2\cdot r_z(0)\cdot[r_z(0)-|r_z(n_0)|]\end{aligned} \tag{A.2}$$

for all n. We can see, from (A.2), that if $r_z(0)=|r_z(n_0)|$, then

$$r_z(n)=\text{sign}(r_z(n_0))\cdot r_z(n+n_0) \tag{A.3}$$

which implies that $r_z(n)$ is a periodic function with period equal to either n_0 when $r_z(n_0)>0$ or $2n_0$ when $r_z(n_0)<0$. **Q.E.D.**

Appendix B
Proof of Property 1

By (18) and Parseval's relation, the denominator of $J_{2,m}$ given by (5) can be shown to be

$$\begin{aligned}&|C_2\{e(n)\}|^m \\ &\quad=\left|\frac{1}{2\pi}\int_{-\pi}^{\pi}\left\{\sigma_u^2\cdot|G(\omega)|^2+\sigma_\eta^2\cdot\frac{|G(\omega)|^2}{|F(\omega)|^2}\right\}d\omega\right|^m.\end{aligned} \tag{B.1}$$

We can see, from (B.1), that $|C_2\{e(n)\}|^m$ is dependent on the magnitude response $|G(\omega)|$ but independent of the phase response $\Phi(\omega)$ of the overall system $g(n)$. On the other hand, $|C_m\{e(n)\}|$ in the numerator of $J_{2,m}$ given by (5) has been shown to satisfy the inequality [37]

$$\begin{aligned}|C_m\{e(n)\}| \leq \left(\frac{1}{2\pi}\right)^{m-1}\cdot|\gamma_m| \\ \cdot\left\{\int_{-\pi}^{\pi}\cdots\int_{-\pi}^{\pi}|G(\omega_1)|\cdots|G(\omega_{m-1})| \right. \\ \left.\cdot\,|G(\omega_1+\cdots+\omega_{m-1})|\,d\omega_1\cdots d\omega_{m-1}\right\}\end{aligned} \tag{B.2}$$

and the equality of (B.2) holds if and only if $\Phi(\omega)$ is linear for $-\pi\leq\omega<\pi$, i.e.,

$$\Phi(\omega)=-\omega\xi+\kappa, \qquad -\pi\leq\omega<\pi \tag{B.3}$$

where ξ and κ are constants.

Because $g(n)$ is real

$$\Phi(-\omega)=-\Phi(\omega)+2\pi L, \qquad -\pi\leq\omega<\pi \tag{B.4}$$

where L is an integer. By (B.3) and (B.4), we therefore have $\kappa=\pi L$. Thus, we have completed the proof that $\Phi(\omega)$ is given by (22), regardless of what $|G(\omega)|$ is. **Q.E.D**

Appendix C
Proof of Property 3

Taking partial derivative of $J_{2,m}$ given by (20) and (21) with respect to the overall system coefficient $g(k)$ (where $k=\cdots,-1,0,1,\cdots$) gives rise to

$$\begin{aligned}\frac{\partial J_{2,m}}{\partial g(k)}=2m\cdot J_{2,m}\cdot\left\{\frac{g^{m-1}(k)}{\sum_n g^m(n)}\right. \\ \left.-\frac{\sigma_u^2\cdot g(k)+\sigma_\eta^2\sum_n[f_{\rm I}(n)*g(n)]\cdot f_{\rm I}(n-k)}{\sigma_u^2\sum_n g^2(n)+\sigma_\eta^2\sum_n[f_{\rm I}(n)*g(n)]^2}\right\}.\end{aligned} \tag{C.1}$$

Setting (C.1) to zero yields

$$\frac{g^{m-1}(k)}{\sum_n g^m(n)}=\frac{\sigma_u^2\cdot g(k)+\sigma_\eta^2\sum_n[f_{\rm I}(n)*g(n)]\cdot f_{\rm I}(n-k)}{\sigma_u^2\sum_n g^2(n)+\sigma_\eta^2\sum_n[f_{\rm I}(n)*g(n)]^2} \tag{C.2}$$

and then taking the Fourier transform of (C.2) with respect to the index k leads to

$$\frac{G^{(m-1)}(\omega)}{\sum_n g^m(n)}=\frac{\sigma_u^2\cdot G(\omega)+\sigma_\eta^2\cdot\dfrac{G(\omega)}{|F(\omega)|^2}}{\sigma_u^2\sum_n g^2(n)+\sigma_\eta^2\sum_n[f_{\rm I}(n)*g(n)]^2} \tag{C.3}$$

where $G^{(m-1)}(\omega)$ is defined as (28). From (C.3) and (14), we can easily obtain the result given by (27), where

$$\beta=\frac{\sigma_u^2\sum_n g^2(n)+\sigma_\eta^2\sum_n[f_{\rm I}(n)*g(n)]^2}{\sigma_u^2\sum_n g^m(n)}\neq 0 \tag{C.4}$$

is a constant. **Q.E.D.**

APPENDIX D
INFERENCE OF PROPERTY 4

It can be inferred, from (23) and (26), that as SNR or the bandwidth of $f(n)$ is increased

$$g_{\mathrm{ZP}}(n) \to \tilde{\beta} \cdot [g_{\mathrm{ZP}}(n)]^{m-1} \tag{D.1}$$

since $g_{\mathrm{MSE}}(n) \to \delta(n)$ by R3), where $\tilde{\beta} = \beta \cdot \exp[j\pi L(m-2)]$ is a constant. Equation (D.1) indicates that

$$[g_{\mathrm{ZP}}(n)]^{m-2} \to \begin{cases} 1/\tilde{\beta}, & \text{if } g_{\mathrm{ZP}}(n) \neq 0 \\ 0, & \text{if } g_{\mathrm{ZP}}(n) = 0 \end{cases} \tag{D.2}$$

which together with the fact that $g_{\mathrm{ZP}}(n)$ is stable zero-phase [see (23)] implies that

$$g_{\mathrm{ZP}}(n) \to \frac{1}{\tilde{\beta}^{1/(m-2)}} \left\{ \delta(n) + \sum_{i=1}^{K} [\delta(n-k_i) + \delta(n+k_i)] \right\} \tag{D.3}$$

where k_i and K are non-negative integers. Furthermore, from (D.3) and (24), we can infer that

$$g_{\mathrm{ZP}}(n) \to \frac{1}{\tilde{\beta}^{1/(m-2)}} \cdot \delta(n) \tag{D.4}$$

[i.e., $K = 0$ in (D.3)] as SNR or the bandwidth of $f(n)$ is increased. It then follows, from (D.4) and (26), that

$$g_{\mathrm{ZP}}(n) = \tilde{\beta} \cdot [g_{\mathrm{ZP}}(n)]^{m-1} * g_{\mathrm{MSE}}(n) \to \frac{1}{\tilde{\beta}^{1/(m-2)}} \cdot g_{\mathrm{MSE}}(n). \tag{D.5}$$

As a result, we conclude that $g(n) \to g_{\mathrm{MSE}}(n)$ (except for a scale factor and a time delay) as SNR or the bandwidth of $f(n)$ is increased.

On the other hand, as the cumulant order m is increased

$$[g_{\mathrm{ZP}}(n)]^{m-1} \to [g_{\mathrm{ZP}}(0)]^{m-1} \cdot \delta(n) \tag{D.6}$$

due to (24). From (D.6) and (26), we can infer that as the cumulant order m is increased

$$\begin{aligned} g_{\mathrm{ZP}}(n) &= \tilde{\beta} \cdot [g_{\mathrm{ZP}}(n)]^{m-1} * g_{\mathrm{MSE}}(n) \\ &\to \tilde{\beta} \cdot [g_{\mathrm{ZP}}(0)]^{m-1} \cdot g_{\mathrm{MSE}}(n). \end{aligned} \tag{D.7}$$

In other words, we have inferred the statement of Property 4.

APPENDIX E
PROOF OF F1)

When $f(n)$ is an allpass system, $|F(\omega)| = c$ (a positive constant), then

$$\begin{aligned} \sum_n [f_{\mathrm{I}}(n) * g(n)]^2 &= \frac{1}{2\pi} \int_{-\pi}^{\pi} \frac{|G(\omega)|^2}{|F(\omega)|^2}\, d\omega \\ &= \frac{1}{c^2} \cdot \frac{1}{2\pi} \int_{-\pi}^{\pi} |G(\omega)|^2 d\omega \\ &= \frac{1}{c^2} \sum_n g^2(n). \end{aligned} \tag{E.1}$$

By (20) and (E.1), we have

$$J_{2,m}(g(n)) = \frac{|\gamma_m|^2}{|\sigma_u^2|^m} \cdot R_{2,m}(g(n)) \cdot \frac{1}{\left| 1 + \dfrac{\sigma_\eta^2}{\sigma_u^2} \cdot \dfrac{1}{c^2} \right|^m} \tag{E.2}$$

which, together with R5) and R2), therefore implies the statement of F1). **Q.E.D.**

APPENDIX F
PROOF FOR THE STATEMENT OF R6)

Let $\tilde{\Phi}_i(\omega) = \arg[\tilde{G}_i(\omega)]$ [see (29)] and $\Phi_i(\omega) = \arg[G_i(\omega)]$, where $G_i(\omega)$ is the Fourier transform of $g_i(n)$ given by (30). Suppose that

$$\Phi_{i-1}(\omega) = \arg[G_{i-1}(\omega)] = \omega a + \pi l, \qquad -\pi \le \omega < \pi \tag{F.1}$$

where a is a constant, and l is an integer. Then, what we need to prove is that $\tilde{\Phi}_i(\omega)$ has the same form as $\Phi_{i-1}(\omega)$ given by (F.1).

Note that $G_{i-1}^{(m-1)}(\omega)$ [see S2) of Algorithm 1] can be expressed as

$$\begin{aligned} G_{i-1}^{(m-1)}(\omega) &= \overbrace{G_{i-1}(\omega) * G_{i-1}(\omega) \cdots * G_{i-1}(\omega)}^{(m-1)\text{ terms}} \\ &= \left(\frac{1}{2\pi}\right)^{m-2} \int_{-\pi}^{\pi} \cdots \int_{-\pi}^{\pi} |G_{i-1}(\Omega_1)| \\ &\quad \cdots |G_{i-1}(\Omega_{m-2})| \cdot |G_{i-1}(\omega - \sum_{k=1}^{m-2} \Omega_k)| \\ &\quad \cdot \exp\left\{ j \left[\Phi_{i-1}(\Omega_1) + \cdots + \Phi_{i-1}(\Omega_{m-2}) \right.\right. \\ &\quad \left.\left. + \Phi_{i-1}\left(\omega - \sum_{k=1}^{m-2} \Omega_k\right) \right] \right\} d\Omega_1 \cdots d\Omega_{m-2}. \end{aligned} \tag{F.2}$$

By (F.1) and (F.2), $\tilde{G}_i(\omega)$ given by (29) can be shown to be

$$\begin{aligned} \tilde{G}_i(\omega) = &\left\{ \left(\frac{1}{2\pi}\right)^{m-2} \int_{-\pi}^{\pi} \cdots \int_{-\pi}^{\pi} |G_{i-1}(\Omega_1)| \right. \\ &\cdots |G_{i-1}(\Omega_{m-2})| \\ &\left. \cdot \left| G_{i-1}\left(\omega - \sum_{k=1}^{m-2} \Omega_k\right) \right| d\Omega_1 \cdots d\Omega_{m-2} \right\} \\ &\cdot G_{\mathrm{MSE}}(\omega) \cdot \exp\{j[\omega a + \pi l(m-1)]\} \end{aligned} \tag{F.3}$$

which implies that

$$\tilde{\Phi}_i(\omega) = \arg[\tilde{G}_i(\omega)] = \omega a + \pi l(m-1), \qquad -\pi \le \omega < \pi \tag{F.4}$$

since $G_{\mathrm{MSE}}(\omega) \ge 0$ [see (13)]. From (30), it follows that $\Phi_i(\omega) = \tilde{\Phi}_i(\omega)$. This, together with (F.1) and (F.4), indicates that if $g_{i-1}(n)$ is linear phase, then $g_i(n)$ is also linear phase. As a consequence, $g(n)$ obtained by Algorithm 1 is linear phase as long as $g_0(n)$ is linear phase. Meanwhile, Property 2 can also be applied to the obtained $g(n)$ because it was deduced from (22). **Q.E.D.**

APPENDIX G
PROOF OF F2) AND F3)

A. Proof of F2)

Since $g(n) = \delta(n)$ for the ZF equalizer, ρ_{ZF} given by (31) can be easily shown to be

$$\begin{aligned}\rho_{\text{ZF}} &= \frac{\sum_n b^2(n)}{\sum_n h^2(n) \cdot \sum_n f_{\text{I}}^2(n)} \\ &= \frac{\frac{1}{2\pi}\int_{-\pi}^{\pi} |B(\omega)|^2 d\omega}{\frac{1}{2\pi}\int_{-\pi}^{\pi} |H(\omega)|^2\, d\omega \cdot \frac{1}{2\pi}\int_{-\pi}^{\pi} \frac{|B(\omega)|^2}{|H(\omega)|^2}\, d\omega} \\ &\quad \text{[by (19)]}. \end{aligned} \tag{G.1}$$

If $w(n)$ is white, $|B(\omega)| = c$ (a positive constant) due to (7), and then

$$\rho_{\text{ZF}} = \frac{1}{\frac{1}{2\pi}\int_{-\pi}^{\pi} |H(\omega)|^2\, d\omega \cdot \frac{1}{2\pi}\int_{-\pi}^{\pi} \frac{1}{|H(\omega)|^2}\, d\omega}. \tag{G.2}$$

By the Cauchy–Schwartz inequality

$$\begin{aligned}&\int_{-\pi}^{\pi} |H(\omega)|^2\, d\omega \cdot \int_{-\pi}^{\pi} \frac{1}{|H(\omega)|^2}\, d\omega \\ &\quad \ge \left[\int_{-\pi}^{\pi} |H(\omega)| \cdot \frac{1}{|H(\omega)|}\, d\omega\right]^2 = (2\pi)^2 \end{aligned} \tag{G.3}$$

which, together with (G.2), therefore leads to $\rho_{\text{ZF}} \le 1$.

On the other hand, if $b(n)$ is not an allpass system [i.e., $w(n)$ is colored], it is possible that $\rho_{\text{ZF}} > 1$. To show this, let us consider the following case. Suppose that $H(\omega) = 1 + e^{j\omega}$ and $B(\omega) = |H(\omega)|^2 = 2(1 + \cos\omega) \ge 0$. Note that $B(\omega) = |B(\omega)|$ and that $b(0) = 2$ and $b(1) = b(-1) = 1$. Then, by (G.1), we have

$$\rho_{\text{ZF}} = \frac{\frac{1}{2\pi}\int_{-\pi}^{\pi} B^2(\omega)\, d\omega}{\left[\frac{1}{2\pi}\int_{-\pi}^{\pi} B(\omega)\, d\omega\right]^2} = \frac{\sum_n b^2(n)}{b^2(0)} = 1.5 > 1. \tag{G.4}$$

This therefore completes the proof of F2).

B. Proof of F3)

Let $\mathcal{J}_{\text{MSE}}(g(n))$ denote the mean square error as

$$\mathcal{J}_{\text{MSE}}(g(n)) \triangleq E\{[u(n) - c(n)]^2\}. \tag{G.5}$$

Using the principle of orthogonality [3], [4], we can easily show that the minimum value of $\mathcal{J}_{\text{MSE}}(g(n))$ is given by

$$\begin{aligned}\mathcal{J}_{\text{MSE}}(g(n) = g_{\text{MSE}}(n)) &= \sigma_u^2 \cdot \{1 - g_{\text{MSE}}(0)\} \\ &= \sigma_u^2 \cdot \left\{1 - \frac{g_{\text{MSE}}^2(0)}{g_{\text{MSE}}(0)}\right\} \end{aligned} \tag{G.6}$$

since $g_{\text{MSE}}(0) \ne 0$ [see (16)]. From (14), we have

$$\begin{aligned}1 &= G_{\text{MSE}}(\omega) \cdot \frac{\sigma_u^2 \cdot |F(\omega)|^2 + \sigma_\eta^2}{\sigma_u^2 \cdot |F(\omega)|^2} \\ &= G_{\text{MSE}}(\omega) + \frac{\sigma_\eta^2}{\sigma_u^2} \cdot \frac{G_{\text{MSE}}(\omega)}{F(\omega)} \cdot \frac{1}{F^*(\omega)}. \end{aligned} \tag{G.7}$$

Taking the inverse Fourier transform of (G.7) yields

$$\delta(k) = g_{\text{MSE}}(k) + \frac{\sigma_\eta^2}{\sigma_u^2} \sum_n [f_{\text{I}}(n) * g_{\text{MSE}}(n)] \cdot f_{\text{I}}(n-k) \tag{G.8}$$

which further leads to

$$\begin{aligned}g_{\text{MSE}}(0) &= \sum_k \delta(k) g_{\text{MSE}}(k) \\ &= \sum_k g_{\text{MSE}}^2(k) + \frac{\sigma_\eta^2}{\sigma_u^2} \sum_n [f_{\text{I}}(n) * g_{\text{MSE}}(n)]^2. \end{aligned} \tag{G.9}$$

Thus, by (G.6) and (G.9), we obtain (G.10), shown at the bottom of the page.

On the other hand, by (8) and A4), $\mathcal{J}_{\text{MSE}}(g(n))$ given by (G.5) can be further expressed as

$$\begin{aligned}\mathcal{J}_{\text{MSE}}(g(n)) &= E\{u^2(n)\} + E\{e_{\text{S}}(n)^2\} + E\{w'(n)^2\} \\ &\quad - 2 \cdot E\{u(n) e_{\text{S}}(n)\} \\ &= \sigma_u^2 + \sigma_u^2 \sum_n g^2(n) + \sigma_\eta^2 \sum_n [f_{\text{I}}(n) * g(n)]^2 \\ &\quad - 2\sigma_u^2 \cdot g(0) \quad \text{[by (18)]}. \end{aligned} \tag{G.11}$$

$$\begin{aligned}\mathcal{J}_{\text{MSE}}(g_{\text{MSE}}(n)) &= \sigma_u^2 \cdot \left\{1 - \frac{g_{\text{MSE}}^2(0)}{\sum_k g_{\text{MSE}}^2(k) + \frac{\sigma_\eta^2}{\sigma_u^2} \sum_n [f_{\text{I}}(n) * g_{\text{MSE}}(n)]^2}\right\} \\ &= \sigma_u^2 \cdot \left\{1 - \frac{g_{\text{MSE}}^2(0)}{\sum_k g_{\text{MSE}}^2(k)} \cdot \frac{1}{1 + \frac{1}{\rho_{\text{MSE}} \cdot \text{SNR}}}\right\} \quad \text{[by (33) and (31)]}. \end{aligned} \tag{G.10}$$

$$g(n)=\frac{\delta(n)}{1+\dfrac{\sigma_\eta^2}{\sigma_u^2}\displaystyle\sum_n f_{\mathrm{I}}^2(n)}=\frac{\delta(n)}{1+\dfrac{1}{\rho_{\mathrm{ZF}}\cdot\mathrm{SNR}}}$$
[by (33) and (31)] (G.12)

(associated with the ZF equalizer) into (G.11) yields

$$\begin{aligned}
&\mathcal{J}_{\mathrm{MSE}}\left(\frac{\delta(n)}{1+\dfrac{\sigma_\eta^2}{\sigma_u^2}\displaystyle\sum_n f_{\mathrm{I}}^2(n)}\right)\\
&\quad=\sigma_u^2\cdot\left\{1-\frac{1}{1+\dfrac{\sigma_\eta^2}{\sigma_u^2}\displaystyle\sum_n f_{\mathrm{I}}^2(n)}\right\}\\
&\quad=\sigma_u^2\cdot\left\{1-\frac{1}{1+\dfrac{1}{\rho_{\mathrm{ZF}}\cdot\mathrm{SNR}}}\right\}\\
&\quad\geq\mathcal{J}_{\mathrm{MSE}}(g_{\mathrm{MSE}}(n))\\
&\quad=\sigma_u^2\cdot\left\{1-\frac{g_{\mathrm{MSE}}^2(0)}{\displaystyle\sum_k g_{\mathrm{MSE}}^2(k)}\cdot\frac{1}{1+\dfrac{1}{\rho_{\mathrm{MSE}}\cdot\mathrm{SNR}}}\right\}.
\end{aligned}\tag{G.13}$$

Since $g_{\mathrm{MSE}}^2(0)\leq\Sigma_k\, g_{\mathrm{MSE}}^2(k)$, (G.13) implies that $\rho_{\mathrm{MSE}}\geq\rho_{\mathrm{ZF}}$. **Q.E.D.**

Appendix H
Proof of Property 5

By (34), the optimum $g(n)$ associated with the maximum of $J_{2,m}$ satisfies

$$\begin{aligned}
J_{2,m}(g(n),\rho_{2,m})&=\frac{|\gamma_m|^2}{|\sigma_u^2|^m}\cdot R_{2,m}(g(n))\cdot\frac{1}{\left|1+\dfrac{1}{\rho_{2,m}\cdot\mathrm{SNR}}\right|^m}\\
&\geq J_{2,m}(g(n)=\delta(n),\rho_{2,m}=\rho_{\mathrm{ZF}})\\
&=\frac{|\gamma_m|^2}{|\sigma_u^2|^m}\cdot\frac{1}{\left|1+\dfrac{1}{\rho_{\mathrm{ZF}}\cdot\mathrm{SNR}}\right|^m}
\end{aligned}\tag{H.1}$$

where $R_{2,m}(g(n)=\delta(n))=1$ [see R5)] has been used in the derivation of (H.1). By (H.1) and the fact that $R_{2,m}(g(n))\leq 1$ [see R5)], the result that $\rho_{2,m}\geq\rho_{\mathrm{ZF}}$ can be obtained. **Q.E.D.**

Appendix I
Inference of Property 7

Let $\mathrm{SNR_H}$ and $\mathrm{SNR_L}$ be two different values of SNR and $\mathrm{SNR_H}>\mathrm{SNR_L}$. Additionally, let $(g_{\mathrm{H}}(n),\rho_{2,m}^{(\mathrm{H})})$ and $(g_{\mathrm{L}}(n),\rho_{2,m}^{(\mathrm{L})})$ be the optimum solutions to the maximum of $J_{2,m}$ given by (34) for $\mathrm{SNR}=\mathrm{SNR_H}$ and $\mathrm{SNR}=\mathrm{SNR_L}$, respectively. From (34), it follows that when $\mathrm{SNR}=\mathrm{SNR_L}$ 4

$$\begin{aligned}
&J_{2,m}(g_{\mathrm{L}}(n),\rho_{2,m}^{(\mathrm{L})})\\
&\quad=\frac{|\gamma_m|^2}{|\sigma_u^2|^m}\cdot R_{2,m}(g_{\mathrm{L}}(n))\\
&\qquad\cdot\frac{1}{\left|1+\dfrac{1}{\rho_{2,m}^{(\mathrm{L})}\cdot\mathrm{SNR_L}}\right|^m}\geq J_{2,m}(g_{\mathrm{H}}(n),\rho_{2,m}^{(\mathrm{H})})\\
&\quad=\frac{|\gamma_m|^2}{|\sigma_u^2|^m}\cdot R_{2,m}(g_{\mathrm{H}}(n))\cdot\frac{1}{\left|1+\dfrac{1}{\rho_{2,m}^{(\mathrm{H})}\cdot\mathrm{SNR_L}}\right|^m}.
\end{aligned}\tag{I.1}$$

From (D.4) in Appendix D, we can infer that $g_{\mathrm{H}}(n)$ is closer to $\delta(n)$ (except for a scale factor and a time delay) than is $g_{\mathrm{L}}(n)$ since $\mathrm{SNR_H}>\mathrm{SNR_L}$ and further infer that $R_{2,m}(g_{\mathrm{H}}(n))\geq R_{2,m}(g_{\mathrm{L}}(n))$ by R5). Therefore, from (I.1) and the result of $R_{2,m}(g_{\mathrm{H}}(n))\geq R_{2,m}(g_{\mathrm{L}}(n))$, we can obtain

$$\rho_{2,m}^{(\mathrm{H})}\leq\rho_{2,m}^{(\mathrm{L})}.\tag{I.2}$$

In other words, the ratio $\rho_{2,m}$ always increases as SNR decreases.

Acknowledgment

The authors appreciate the anonymous reviewers for their valuable comments and suggestions on the improvement of the paper.

References

[1] J. Makhoul, "Linear prediction: A tutorial review," *Proc. IEEE*, vol. 63, pp. 561–580, Apr. 1975.
[2] S. M. Kay, *Modern Spectral Estimation*. Englewood Cliffs, NJ: Prentice-Hall, 1988.
[3] C. W. Therrien, *Discrete Random Signals and Statistical Signal Processing*. Englewood Cliffs, NJ: Prentice-Hall, 1992.
[4] M. H. Hayes, *Statistical Digital Signal Processing and Modeling*. New York: Wiley, 1996.
[5] C.-Y. Chi and M.-C. Wu, "A unified class of inverse filter criteria using two cumulants for blind deconvolution and equalization," *Proc. IEEE 1995 Int. Conf. Acoust., Speech, Signal Process.*, Detroit, MI, May 9–12, 1995, pp. 1960–1963.
[6] ——, "Inverse filter criteria for blind deconvolution and equalization using two cumulants," *Signal Process.*, vol. 43, no. 1, pp. 55–63, Apr. 1995.
[7] J. A. Cadzow, "Blind deconvolution via cumulant extrema," *IEEE Signal Processing Mag.*, vol. 13, pp. 24–42, May 1996.
[8] R. A. Wiggins, "Minimum entropy deconvolution," *Geoexplor.*, vol. 16, pp. 21–35, 1978.
[9] D. L. Donoho, "On minimum entropy deconvolution," *Applied Time Series Analysis II*, D. F. Findly, Ed. New York: Academic, 1981.
[10] J. K. Tugnait, "Estimation of linear parametric models using inverse filter criteria and higher order statistics," *IEEE Trans. Signal Processing*, vol. 41, pp. 3196–3199, Nov. 1993.
[11] O. Shalvi and E. Weinstein, "New criteria for blind deconvolution of nonminimum phase systems (channels)," *IEEE Trans. Inform. Theory*, vol. 36, pp. 312–321, Mar. 1990.
[12] S. Haykin, Ed. *Blind Deconvolution*. Englewood Cliffs, NJ: Prentice-Hall, 1994.
[13] J. A. Cadzow and X. Li, "Blind deconvolution," *Digital Signal Process. J.*, vol. 5, no. 1, pp. 3–20, Jan. 1995.
[14] G. B. Giannakis and J. M. Mendel, "Identification of nonminimum phase system using higher order statistics," *IEEE Trans. Acoust., Speech, Signal Processing*, vol. 37, pp. 360–377, Mar. 1989.

[15] ———, "Cumulant-based order determination of nongaussian ARMA models," *IEEE Trans. Acoust., Speech, Signal Processing*, vol. 38, pp. 1411–1423, Aug. 1990.
[16] G. B. Giannakis and A. Swami, "On estimating noncausal nonminimum phase ARMA models of nongaussian processes," *IEEE Trans. Acoust., Speech, Signal Processing*, vol. 38, pp. 478–495, Mar. 1990.
[17] D. Godard, "Self recovering equalization and carrier tracking in two-dimensional data communication systems," *IEEE Trans. Commun.*, vol. COMM-28, pp. 1867–1875, Nov. 1980.
[18] M. Ooe and T. J. Ulrych, "Minimum entropy deconvolution with an exponential transformation," *Geophys. Prospect.*, vol. 27, pp. 458–473, 1979.
[19] A. Ziolkowski, *Deconvolution*. Boston, MA: Int. Human Res. Development Corp., 1984.
[20] J. M. Mendel, "Tutorial on higher-order statistics (spectra) in signal processing and system theory: Theoretical results and some applications," *Proc. IEEE*, vol. 79, pp. 278–305, Mar. 1991.
[21] C. L. Nikias and J. M. Mendel, "Signal processing with higher-order statistics," *IEEE Signal Processing Mag.*, vol. 10, pp. 10–37, July 1993.
[22] C. L. Nikias and A. P. Petropulu, *Higher-Order Spectra Analysis*. Englewood Cliffs, NJ: Prentice-Hall, 1993.
[23] M. S. Bartlett, *An Introduction to Stochastic Processes*. London, U.K.: Cambridge Univ. Press, 1955.
[24] D. R. Brillinger, *Time Series, Data Analysis, and Theory*. New York: Holt, Rinehart, and Winston, 1975.
[25] D. R. Brillinger and M. Rosenblatt, "Computation and interpretation of kth-order spectra," in *Spectral Analysis of Time Series*, B. Harris, Ed. New York: Wiley, 1967, pp. 189–232.
[26] J. G. Proakis, *Digital Communications*. Singapore: McGraw-Hill, 1995.
[27] J. M. Mendel, "White-noise estimators for seismic data processing in oil exploration," *IEEE Trans. Automat. Contr.*, vol. AC-22, pp. 694–706, 1977.
[28] ———, "Single-channel white-noise estimators for deconvolution," *Geophys.*, vol. 43, no. 1, pp. 102–124, Feb. 1978.
[29] ———, "Minimum-variance deconvolution," *IEEE Trans. Geosci. Remote Sensing*, vol. GE-19, pp. 161–171, 1981.
[30] C.-Y. Chi and J. M. Mendel, "Performance of minimum-variance deconvolution filter," *IEEE Trans. Acoust., Speech, Signal Processing*, vol. ASSP-32, pp. 1145–1153, Dec. 1984.
[31] C.-Y. Chi, "A further analysis for the minimum-variance deconvolution filter performance," *IEEE Trans. Acoust., Speech, Signal Processing*, vol. 35, pp. 888–889, June 1987.
[32] D. M. Burley, *Studies in Optimization*. New York: Falsted, 1974.
[33] J. Kormylo and J. M. Mendel, "Maximum-likelihood deconvolution," *IEEE Trans. Geosci. Remote Sensing*, vol. GE-21, pp. 72–82, 1983.
[34] C.-Y. Chi, J. M. Mendel, and D. Hampson, "A computationally fast approach to maximum-likelihood deconvolution," *Geophys.*, vol. 49, no. 5, pp. 550–565, May 1984.
[35] J. M. Mendel, *Optimal Seismic Deconvolution: An Estimation-Based Approach*. New York: Academic, 1983.
[36] ———, *Maximum-Likelihood Deconvolution: A Journey into Model-Based Signal Processing*. New York: Springer-Verlag, 1990.
[37] H.-M. Chien, H.-L. Yang, and C.-Y. Chi, "Parametric cumulant based phase estimation of 1-D and 2-D nonminimum phase systems by allpass filtering," *IEEE Trans. Signal Processing*, vol. 45, pp. 1742–1762, July 1997.
[38] D. G. Luenberger, *Linear and Nonlinear Programming*. Reading, MA: Addison-Wesley, 1984.

Chih-Chun Feng (S'97) was born in Taiwan, R.O.C., on August 14, 1969. He received the B.S. degree in electronic engineering from Feng Chia University, Taichung, Taiwan, in 1992 and the M.S. degree in communication engineering from National Chiao Tung University, Hsinchu, Taiwan, in 1994. He is currently working toward the Ph.D. degree in electrical engineering at National Tsing Hua University, Hsinchu.

His research interests include statistical signal processing, higher order statistical analysis, system identification and estimation, blind deconvolution, and wireless communications.

Chong-Yung Chi (S'83–M'83–SM'89) was born in Taiwan, R.O.C., on August 7, 1952. He received the B.S. degree from the Tatung Institute of Technology, Taipei, Taiwan, in 1975, the M.S. degree from the National Taiwan University, Taipei, in 1977, and the Ph.D. degree from the University of Southern California, Los Angeles, in 1983, all in electrical engineering.

From July 1983 to September 1988, he was with the Jet Propulsion Laboratory, Pasadena, CA, where he worked on the design of various spaceborne radar remote sensing systems including radar scatterometers, SAR's, altimeters, and rain mapping radars. From October 1988 to July 1989, he was a Visiting Specialist at the Department of Electrical Engineering, National Taiwan University. Since August 1989, he has been a Professor with the Department of Electrical Engineering, National Tsing Hua University, Hsinchu, Taiwan. He has published more than 80 technical papers in radar remote sensing, system identification and estimation theory, deconvolution and channel equalization, digital filter design, spectral estimation, and higher order statistics (HOS) based signal processing. His research interests include signal processing for wireless communications, statistical signal processing, and digital signal processing and their applications.

Dr. Chi has served as a reviewer for several international journals and conferences, such as the IEEE TRANSACTIONS ON SIGNAL PROCESSING, the IEEE TRANSACTIONS CIRCUITS AND SYSTEMS, the IEEE TRANSACTIONS ON GEOSCIENCE AND REMOTE SENSING, and *Electronic Letters*, since 1983. He is also an active member of New York Academy of Sciences, an active member of the Society of Exploration Geophysicists, a member of the European Association for Signal Processing, and an active member of the Chinese Institute of Electrical Engineering. He is also a technical committee member of both 1997 and 1999 IEEE Signal Processing Workshop on Higher Order Statistics.